

CHEMOPREVENTION EFFICACY OF INDOLE-3-CARBINOL IN EXPERIMENTALLY INDUCED HAMSTER BUCCAL POUCH CARCINOGENESIS

Kamal Abdelrahman Kamal* and Magdi A. Alazazi**

ABSTRACT

Abstract: The aim of the present study was directed to investigate the effect of indole-3-carbinol (I3C) as a new chemopreventive modality in experimentally induced hamster buccal pouch (HBP) carcinogenesis. **Material and methods:** Twenty five golden Syrian male hamsters five weeks old, weighting 80-120 gs were used as experimental animals and divided into three group_(s) (G_(s)) (G1, G2 and G3): G1 (negative control): 5 animals were left untreated. G2: (dimethylbenz[a]anthracene (DMBA) painting-HBP group): 10 animals, their right buccal pouches were painted with 0.5% DMBA in paraffin oil 3 times a week and divided into two subgroups, G2A and G2B (G2A which included 5 animals and painted for 8 weeks, G2B which included 5 animals and painted for 14 weeks. G3 (I3C chemoprevention group): 10 hamsters were included in this group were received I3C given by the oral route using a specific vehicle one week before, as well as during the application of DMPA on alternative days for 8 weeks (G3A) and for 14 weeks (G3B). After termination of the experiment, all animals were sacrificed, and the buccal mucosa was excised and fixed in 10% neutral buffered formalin, routinely processed and embedded in paraffin blocks for preparation in order to be examined histologically and immunohistochemically and then statistical analysis based on these examinations was done **Results:** Gross observations revealed variable features in (G2 and G3) compared to that observed in group G1 ranging from normal and smooth surface to fungating tumor masses of large sizes. Histopathological findings revealed variations among chemoprevention groups ranging from normal epithelial layers to epithelial dysplasia to squamous cell carcinoma with invading nests and pearls. Immunohistochemical (IHC) results, regarding Bax expression, revealed variability in the area percentage throughout the groups used. At 8 weeks, area percentages of G1, G2A, and G3A were (39.83%, 22.00 %, and 30.47 %) respectively, and at 14 weeks were (39.83%, 10.45 % and 26.19%) respectively. Bcl2 expressions also had variability in the area percentage throughout the same groups at 8 weeks were (7.05 %, 43.09 % and 18.15 %) respectively, while at 14 weeks they were (7.05 %, 75.21 % and 43.76 %) respectively. **Conclusion:** I3C is considered as a promising chemotherapeutic agent in prevention of induced HBP carcinogenesis (epithelial dysplasia & invasive carcinoma) and proved beneficial role in improving the outcome by modulating apoptosis and proliferation throughout the process of carcinogenesis.

Keywords: HBP carcinoma, indole-3-carbinol, Bax, Bcl2.

* Lecturer of Oral and Dental Pathology - Faculty of Dentistry - Al-Azhar University.

** Lecturer of Oral Biology - Faculty of Dentistry - Al-Azhar University.

INTRODUCTION

Head and neck cancer is the sixth most common human cancer ^[1], representing 3% of all types of cancer. They are located in the oral cavity in 48% of cases, and 90% of these are oral squamous cell carcinoma (OSCC) ^[2]. They are sometimes preceded by precancerous lesions, such as leukoplakia and erythroplakia. More than 300,000 new cases of oral squamous cell carcinoma are diagnosed annually ^[3]. Approximately 35,000 new cases are recorded annually in the US ^[2], 40,000 new cases are recorded in the EU and 10915 new cases in Japan ^[4]. The most common site for intraoral carcinoma is the tongue, which accounts for around 40% of all cases in the oral cavity proper. Tongue cancers most frequently occur on the posterior-lateral border and ventral surfaces of the tongue. The floor of the mouth is the second most common intraoral location. Less common sites include the gingival, buccal mucosa, labial mucosa, and hard plate. The incidence of oral cancer has significant local variation. Oral and pharyngeal carcinomas account for up to half of all malignancies in India and other Asian countries, and this particularly high prevalence is attributed to the influence of carcinogens and region-specific epidemiological factors, especially tobacco and chewing betel quid. An increase in the prevalence of oral cancer among young adults is a cause of special concern. There has been a 60% increase in the number of under 40 years olds with tongue cancer over past 30 years. However, little has been published on the etiology and natural history of this increase ^[5].

The concept of multiclonal “field cancerization” is supported by patients with oral cancers who present with multiple primary tumors or secondary tumors ^[6]. Multifocal dysplastic lesions could arise from single site as a result of lateral intraepithelial migration or intraoral dispersion and, with additional genetic changes, acquire a growth advantage ^[7]. The clonal origin of multiple premalignant or

malignant lesions in the same patient is supported by recent cytogenetic findings^[8]. Either a polyclonal or a monoclonal hypothesized origin of multiple oral cancers is consistent with the finding that aneuploidy in only one of several biopsy specimens obtained simultaneously or successively from the same patient can be used to predict subsequent carcinoma occurrence^[9]. Induction of (OSCC) can be successfully done by 7, 12-dimethylbenz[a]anthracene (DMBA) in hamster buccal pouch (HBP). It has been found that induced OSCC closely mimics with that of human on morphological, histological and biochemical aspects as well as at molecular level ^[10]. Surgery and chemotherapy for OSCC have limited efficacy ^[11,12], thus, there is an urgent need to elucidate the mechanisms of development of OSCC and develop a new strategy for its treatment and prevention. Both epidemiological and physiological studies suggest that phytochemicals from vegetables and fruits represent a largely untapped source of potential anticancer molecules^[13,16]. Increased vegetable intake is linked to a reduction in the risk of acquiring several types of cancers ^[17,18]. Within this food group, enhanced consumption of cruciferous vegetables e.g., broccoli, cabbage, cauliflower, bok choy and Brussels spouts) surfaces as a factor associated with a reduction in cancers particularly in the colon, lung, prostate, cervix and breast ^[19–22], although admittedly, considerable controversy exists ^[21]. One such phytochemical is indole-3-carbinol (I3C), an autolysis product of glucosinolates present in Brassica vegetables such as broccoli, cabbage, and cauliflower. Dietary exposure to I3C reduced tumor occurrence and decreased the multiplicity of spontaneous as well as carcinogen-induced mammary tumor formation in rodent model systems ^[23–24]. I3C also tested positive as a chemopreventative agent in several short-term bioassays relevant to carcinogen-induced DNA damage, tumor initiation and promotion, and oxidative stress ^[25].

Dietary indoles has been documented as inhibiting tumorigenesis in various target organs including colon^[26], thyroid^[27], pancreas^[28], liver^[29], cervix^[30], melanoma^[31], and lung^[32]. Several mechanisms may account for the anticancer properties of I3C/ diindolymethane (DIM) including changes in cell cycle progression, apoptosis, carcinogen bioactivation and DNA repair. It remains uncertain as to which of these is most important to bring about the anticancer properties attributed to crucifers and if a common cellular mechanism may account for the observed diverse phenotypic changes^[33]. Clinical trials are planned to test the efficacy of I3C as a preventive treatment for breast cancer^[34]. Laboratory studies suggest that this phytochemical can act in several different ways to prevent transformation and/or tumor progression, as well as to kill transformed cells selectively. I3C is rapidly converted in the stomach to a variety of condensation products, chiefly DIM. Plasma from humans and rats fed I3C contains no detectable I3C, but large amounts of DIM, as well as other metabolites, some of which remain uncharacterized^[35]. It is well documented that nuclear factor (NF- κ B) acts as an important survival factor in cancer cells by mediating the transcription of a series of antiapoptotic genes, including: (B-cell lymphoma 2) Bcl-2, Bcl-xL, survivin, p53, and p21^[36]. In addition, I3C has been shown to activate the stress-induced MAP kinases p38 and c-jun N-terminal kinase (JNK) in prostate cancer cells^[37] and to inhibit constitutively active Signal transducer and activator of transcription 3 (STAT3), a transcription factor, in pancreatic carcinoma cells. Together, the concerted effects on these proapoptotic components underlie the ability of I3C /DIM to induce mitochondria-dependent apoptosis in tumor cells^[38]. This review focuses on the relationships among these anticancer properties and apoptotic events as a function of the quantity and duration of I3C exposure.

MATERIAL AND METHODS

Twenty five golden Syrian male hamsters five weeks old, weighting 80-120gs were obtained from the animal house, Cairo University (Cairo, Egypt). The experimental animals were housed in standard cages with sawdust bedding under controlled environmental conditions of humidity (30-40%), temperature ($20 \pm 2^\circ\text{C}$), and light (12-h light/12-h dark). All experimental animals were supplied with standard diet and water ad libitum. The hamsters were used as model for OSCC induction utilizing 7, 12 DMBA (Sigma-aldrich company) (0.5% in paraffin oil) as chemical carcinogen and I3C was used as chemoprevention agent. The experimental animals were divided into three groups. G1 (negative control): 5 hamsters not treated and served as negative controls. G2 (DMBA painting-HBP group): 10 hamsters were included in this group, the right HPBs of these hamsters were painted with 0.5 DMPA in paraffin (Sigma Aldrich) using a number 4 camel hair brush three times a week and divided into two subgroups, G2A and G2B (G2A which included 5 animals and painted for 8 weeks, G2B which included 5 animals and painted for 14 weeks). G3 (I3C chemoprevention group): 10 hamsters were included in this group were received I3C 50 mg/kg^[39] given by the oral route using a specific vehicle one week before, as well as during the application of DMPA on alternative days for 8 weeks (G3A) and for 14 weeks (G3B).

After termination of the experiment and recording all gross observations and alterations that may happened throughout the experiment, the animals were sacrificed by cervical dislocation, the cheek pouches were excised and fixed in 10% neutral buffered formalin, routinely processed and embedded in paraffin blocks for preparation in order to be examined histologically and immunohistochemically and then statistical analysis based on these examinations was done. For histological examination: The specimens

were dehydrated in an ascending ethanol series, embedded in paraffin wax to form paraffin blocks. Tissue sections using rotary microtome of $4\mu\text{m}$ thickness were cut, mounted on glass slides and stained with hematoxylin and eosin stain (H&E) for light microscopic examination. For immunohistochemical (IHC) examination: Other tissue sections were cut at $4\mu\text{m}$ and put on positive charged slides for the application of standard labeled streptavidin- biotin method to apply each antibody used separately (Bcl-2 and Bax antibodies). Paraffin sections were cut and mounted on positive charged glass slides. Each section was carried into two similar sections one for Bax and one for Bcl-2. The sections were deparaffinized in xylene and rehydrated through graded ethanol (100%, 95% and 70%) each run for 5 minutes. Slides were washed in distilled water then in phosphate buffered saline (PBS), each for 5 minutes.

Endogenous peroxidase activity was blocked using 3% solution of hydrogen peroxide (H_2O_2) in methanol for 30 minutes at room temperature. Slides were then washed in PBS. Slides were then immersed in plastic jars containing 200 ml of 10 M citrate buffer (pH 6) (ready to use from DAKO). The jars were put in microwave at maximum power at 100°C for 3 intervals, each one 5 minutes. Slides were left at room temperature to cool gradually. Slides were then washed in distilled water followed by PBS for 5 minutes. Tissue sections were received one or two drops of the primary antibodies (Bax or Bcl-2) in a dilution of 1:100 and incubated in a humid chamber at room temperature overnight. Slides were then washed in distilled water, followed by PBS for 5 minutes. Biotinylated secondary antibody was added and incubated at room temperature for 30 minutes. Tissue sections were then washed in PBS for 5 minutes. One or two drops of peroxidase-labeled streptavidin were applied for 30 minutes at room temperature then washed in PBS. The tissue sections were received DAB for 2-4 minutes to develop color, followed by putting in

distilled water. Tissue sections were counterstained using Mayer's hematoxylin for one minute and then washed in tap water. The slides were placed in two changes of 95% alcohol followed by two changes of absolute alcohol, each for 3 minutes then mounted with DPX and covered with plastic covers in order to be examined. The immunostained sections were examined using light microscope to assess the prevalence of positive cases and the localization of immunostaining within the tissues. In addition, image analysis computer system was used to assess area percentage of positive cells of the immunostaining. This was done in the Oral and Dental Pathology Department - Faculty of Dental Medicine - Boys- Cairo - Al-Azhar University. The degree of positive staining for each antibody was evaluated by a well-established semi-quantitative scoring on a scale range from negative to strong positive staining as follow: Strong staining (more than 50% stained), moderate staining (between 25 and 50% stained), weak staining (between 5 and 25% stained), and negative (less than 5% stained) ^[40]. Statistical presentation and analysis of the present study was conducted, using the mean, standard deviation, ANOVA and Tukey's test by SPSS V20. Significant level: Non Significant >0.05 Significant <0.05 * High Significant <0.001 *

RESULTS

The gross observation results: HBP mucosae of G1 were pink in color with smooth surface and no observable abnormalities (Table 1, Fig. 1), in G2A, HBP mucosa showed multiple small nodules, area of ulceration and bleeding (Table 1, Fig. 2), in G3A, HBP mucosae showed few small nodules without bleeding or ulceration (Table 1, Fig. 3), in G2B, HBP mucosae showed large size nodular elevations, fungating tumor masses, bleeding and ulceration (Table 2, Fig. 1), in G3B, HBP mucosae showed small nodular elevations with ulcer (Table 2, Fig. 2).

Histopathological and IHC results: In G1, histological sections, using H&E stain, revealed normal HBP mucosae, intact, and continuous epithelium composed of thin keratinized stratified squamous epithelium. Subepithelial connective tissue (C.T), muscular layer and areolar layer were seen (Table 3, Fig. 1). The IHC staining using Bcl-2 showed weak (7.05%) positive expression which limited to basal and suprabasal layers (Table 3, Fig. 2). while Bax expression exhibited moderate (39.83 %) positive expression which present throughout the epithelial layers (Table 3, Fig. 3). Histological sections, using H&E stain of G2A showed 100% incidence of epithelial dysplasia, the overlying

epithelium has obvious, hyperplasia, hyperkeratosis and severe dysplastic features in most epithelial layers in multiple areas including: loss of adhesion, hyperchromatism and abnormal mitosis with intact basement membrane (Table 3, Fig. 4). IHC staining using Bcl-2 expression exhibited moderate (43.09%) positive cytoplasmic expression throughout the dysplastic epithelial layers (Table 3, Fig. 5), also Bax of G2A showed weak (22.00%) positive cytoplasmic expression throughout the dysplastic epithelial layers (Table 3, Fig. 6). Histological sections, using H&E stain of G3A reduced epithelial dysplasia incidence and severity of two premalignant lesions as compared to G2A, hyperkeratosis and mild to

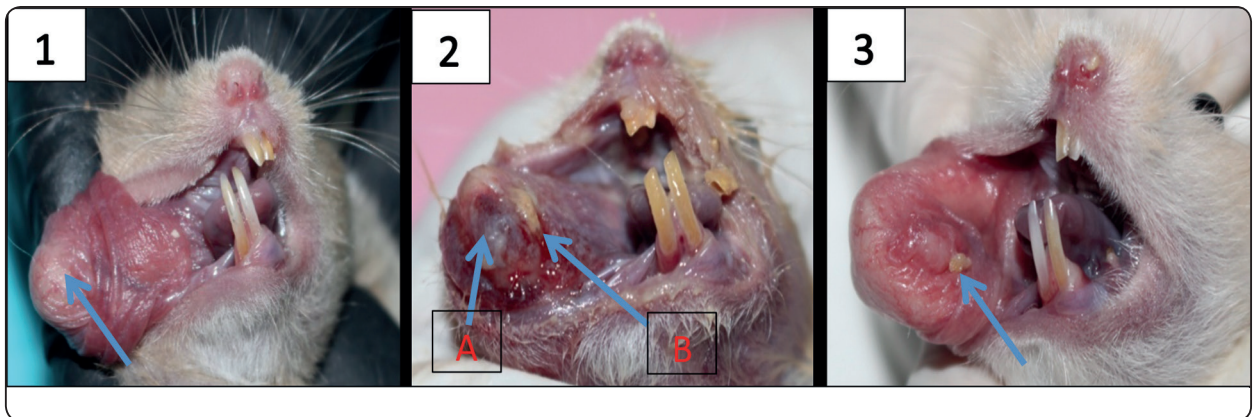


TABLE (1) (Fig.1): HBP of G1 showing normal buccal pouch mucosa which appeared pink in color with smooth surface (arrow). (Fig.2): HBP of G2A, showing multiple small nodules (arrow A), area of ulceration and bleeding (arrow B). (Fig.3): HBP of G3A showing small nodule without bleeding or ulceration (arrow).

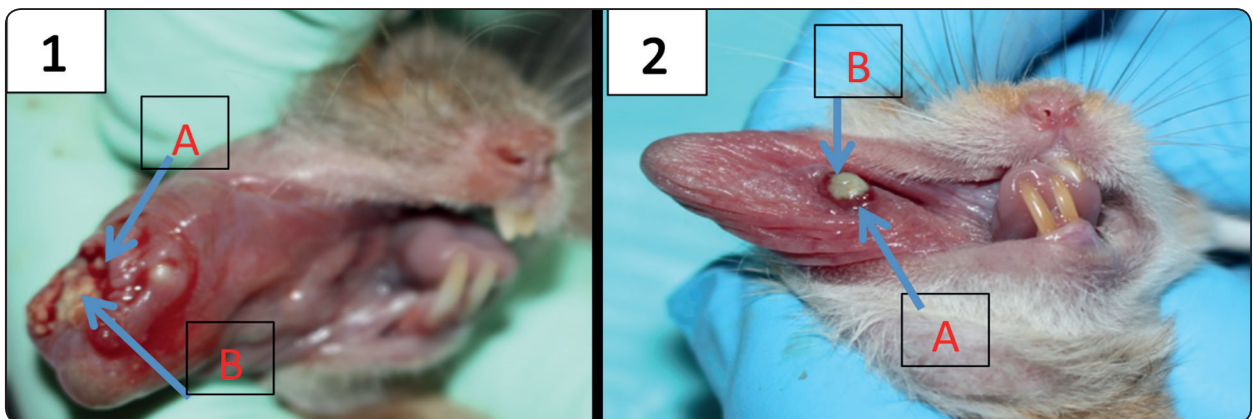


TABLE (2) (Fig.1): HBP of G2B showing large size nodular elevations, fungating tumor masses (arrow A), bleeding and ulceration (arrow B). (Fig.2): HBP of G3B showing small nodular (arrow A), elevations with ulcer (arrow B).

severe dysplastic features in most epithelial layers in multiple areas including: loss of adhesion and abnormal mitosis with intact basement membrane (Table 3, Fig. 7), while three specimen appeared normal almost the same as G1, IHC staining using Bcl-2 expression exhibited weak (18.15%) positive cytoplasmic expression throughout the dysplastic epithelial layers (Table 3, Fig. 8), Bax showed moderate (30.47%) positive cytoplasmic expression throughout the dysplastic epithelial layers (Table 3, Fig. 9).

At 14 weeks: regarding G2B, histological sections, using H&E stain, revealed that 100 % OSCC incidence, the overlying epithelium has obvious dysplastic features in multiple areas with evidence of prominent true invasion. Appearance of various OSCC nests: well differentiated as well as moderately differentiated were observed in the underlying C.T (Table 4, Fig. 1). IHC staining using Bcl-2 expression exhibited strong (75.21%) positive cytoplasmic expression throughout the invading

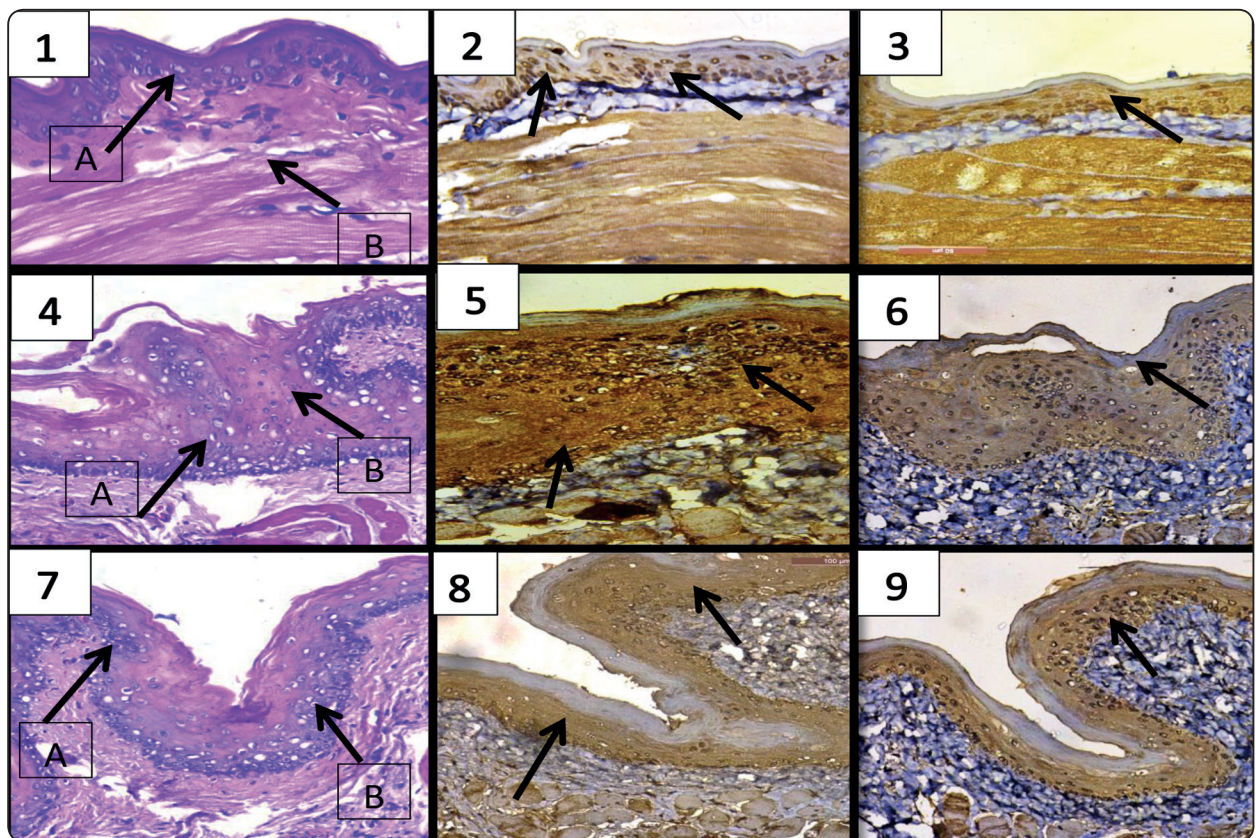


TABLE (3) (Fig.1): H&E stain of G1 showing: intact and continuous epithelium composed of thin keratinized stratified squamous epithelium (arrow A). Subepithelial connective tissue (arrow B). (Fig.2): IHC expression of Bcl-2 showing positive cytoplasmic expression which limited to basal and suprabasal layers (arrows). (Fig.3): IHC expression of Bax showing positive cytoplasmic expression throughout the epithelial layers (arrow). (Fig.4): H&E stain of G2A showing sever epithelial dysplastic features including: abnormal mitosis (arrow A), hyperchromatism and loss of adhesion (arrow B). (Fig.5): IHC expression of Bcl-2 showing positive cytoplasmic expression throughout the dysplastic epithelial layers (arrows). (Fig.6): IHC expression of Bax showing positive cytoplasmic expression throughout the dysplastic epithelial layers (arrow). (Fig.) 7: H&E stain of G3A showing: hyperkeratosis (arrow A) and mild epithelial dysplastic features including: loss of adhesion and abnormal mitosis (arrow B). (Fig.8): IHC expression of Bcl-2 showing positive cytoplasmic expression throughout the dysplastic epithelial layers (arrows). (Fig.9): IHC expression of Bax showing positive cytoplasmic expression throughout the dysplastic epithelial layers (arrow).

nests (Table 4, Fig. 2), Bax showed weak (10.45%) positive cytoplasmic expression throughout the invading nests (Table 4, Fig. 3). Regarding G3B: Simultaneous treatment with I3C and DMBA in G3B significantly reduced OSCC incidence, the overlying epithelium in one animals of G3B (1 of 5) specimens has obvious dysplastic features in multiple areas with evidence of prominent true invasion with formation of epithelial nests, well differentiated SCC nests were observed in the underlying C.T, while other 2 specimens exhibited severe dysplastic features without true invasion and 2 specimens

exhibited mild dysplastic features without true invasion (Table 4, Fig. 4). IHC staining using Bcl-2 expression exhibited moderate (43.76%) positive cytoplasmic expression throughout the invading nests (Table 4, Fig. 5). Bax showed moderate (26.19%) positive cytoplasmic expression throughout the invading nests (Table 4, Fig. 6).

Statistical analysis results of Bcl-2 & Bax expression were obtained by comparing the area % between the groups used. Statistical analysis results were revealed that, in regard to expression

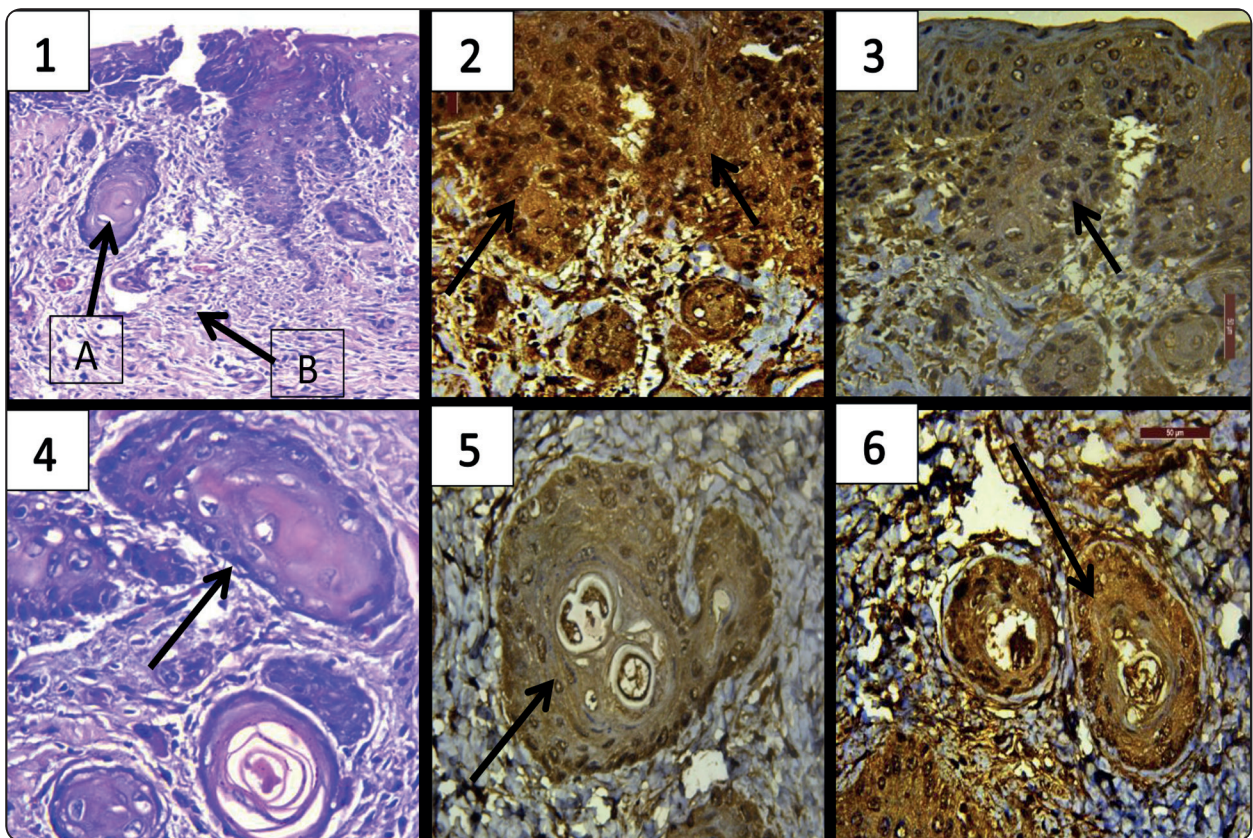


TABLE (4) (Fig.1): H&E stain of G2B showing moderately differentiated OSCC, the overlying epithelium has obvious dysplastic features in multiple areas with evidence of prominent true invasion (arrow A). Subepithelial connective tissue (arrow B). (Fig.2): IHC expression of Bcl-2 showing positive cytoplasmic expression throughout the invasive nests (arrows). (Fig.3): IHC expression of Bax showing positive cytoplasmic expression throughout the invasive nests (arrow). (Fig.4): H&E stain of G2B showing well differentiated OSCC, the overlying epithelium has obvious dysplastic features and multiple areas with epithelial nests with keratin pearls invading the C.T (arrow). (Fig.5): IHC expression of Bcl-2 showing positive cytoplasmic expression throughout the invasive nests (arrow). (Fig.6): IHC expression of Bax showing positive cytoplasmic expression throughout the invasive nests (arrow).

of Bcl-2 at 8 weeks, G2A had recorded the highest mean area percentage (43.09%), while G1 had recorded the lowest mean area percentage (7.05%) and G3A recorded mean area percentage (18.15%) the comparison revealed that there was significant difference between the following (G1 and G2A) and between (G2A and G3A) respectively where P value was (0.005) and there was no significant difference between G1 and G3A where P value was (0.718) (Table 5, Chart 1). While in regard to expression of Bax at 8 weeks, G1 had recorded the highest mean area percentage (39.83%), while G2A had recorded the lowest mean area percentage (22.00 %) and G3A recorded mean area percentage (30.47 %) the comparison revealed that, there was no significant difference between the following (G1 and G2A) , (G1 and G3A) and between (G2A and G3A) respectively where P value was (0.218, 0.774, 0.296), (Table 6, Chart 2). In regard to expression

of Bcl-2 at 14 weeks, G2B had recorded the highest mean area percentage (75.21%), while G1 had recorded the lowest mean area percentage (7.05%) and G3B recorded mean area percentage (43.76%) the comparison revealed that there was significant difference between the following (G1 and G3B) and between (G2B and G3B) respectively where P value was (<0.05) and there was high significant difference between (G1 and G2B) (Table 5, Chart 1). While in regard to expression of Bax at 14 weeks, G1 had recorded the highest mean area percentage (39.83), while G2B had recorded the lowest mean area percentage (10.45 %) and G3B recorded mean area percentage (26.19 %) the comparison revealed that there was significant difference between G1 and G2B, and between G2B and G3B respectively where P value was (<0.05) (Chart 3) and there was no significant difference between G1, G3B where P value was (0.464), (Table 6, Chart 2).

TABLE (5) Mean, standard deviation (SD), P-values and results of comparison between expression of Bcl-2 all groups.

	Bcl-2						ANOVA	
	Range			Mean	±	SD	f	P-value
Group I	3.9	-	12.4	7.05	±	3.26	17.990	<0.001**
Group 2a	24.3	-	61.2	43.09	±	14.21		
Group 2b	63.0	-	94.0	75.21	±	12.76		
Group 3a	13.1	-	23.1	18.15	±	3.98		
Group 3b	13.0	-	66.3	43.76	±	24.07		
Tukey's test								
	Group I		Group 2a		Group 2b		Group 3a	
Group 2a	0.005*							
Group 2b	<0.001**		0.012*					
Group 3a	0.718		0.005*		<0.001**			
Group 3b	0.004*		<0.001**		0.033*		0.060	

TABLE (6) Mean, standard deviation (SD), P-values and results of comparison between expression of Bax all groups.

	Bax						ANOVA	
	Range			Mean	±	SD	f	P-value
Group I	20.9	-	70.3	39.83	±	20.38	3.587	0.023*
Group 2a	10.1	-	31.1	22.00	±	9.78		
Group 2b	5.5	-	18.4	10.45	±	5.94		
Group 3a	19.0	-	50.2	30.47	±	13.83		
Group 3b	11.4	-	34.2	26.19	±	8.88		

Tukey's test				
	Group I	Group 2a	Group 2b	Group 3a
Group 2a	0.218			
Group 2b	0.013*	0.617		
Group 3a	0.774	0.296	0.136	
Group 3b	0.464	0.984	0.011*	0.983

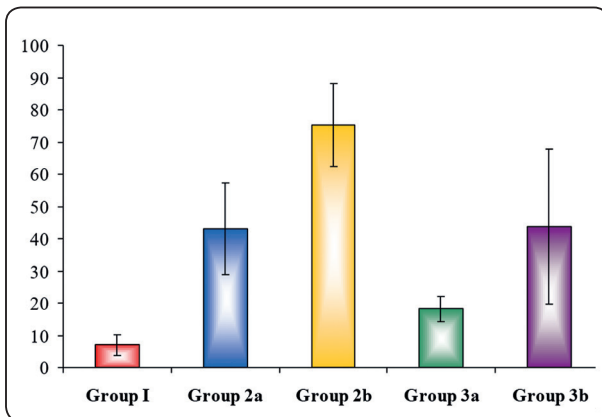


Chart (1): Bar chart representing mean area % results of Bcl-2 expressions in all groups.

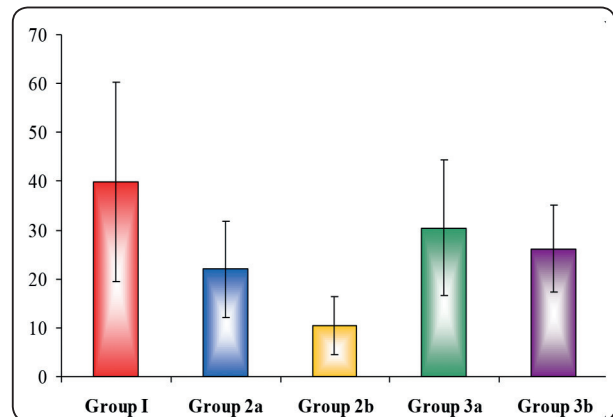


Chart (2): Bar chart representing mean area % results of Bax expressions in all groups.

DISCUSSION

In the present study, the results of the effect of I3C as a new chemopreventive modality in experimentally induced HBP carcinogenesis revealed variable alterations. The development of oral cancer is a multistep process requiring initiation, Promotion and progression. The hamster cheek pouch model is easily developed and can provide one of the most widely accepted experimental models for oral carcinogenesis [41]. Despite the existence of anatomic and histologic variations

between hamster pouch mucosa and human buccal tissue, the DMBA-treated hamster cheek pouch model is able to produce premalignant changes and carcinomas that are similar to the development of disease in human oral mucosa [42]. The changes in histopathological status during DMBA-induced HBP carcinogenesis and their timing in the present study were similar to the results of Kim et al. (2004) [43], Lajolo et al. (2008) [44], and Nishimura et al. (2004) [45]. The results of H&E stain revealed that topical application of DMBA to the HBP for

8 weeks induced severe epithelial dysplasia and for 14 weeks induced invasive SCC. The current results with those of other studies^[46-49] supported the concept that DMBA induced HBP carcinoma appeared to go through the same changes as in human. Many mechanisms have been proposed as etiologic factors in development of DMBA hamster oral carcinoma, such as p53 and K-ras mutations and overexpression of inducible nitric oxide synthase^[50, 51]. In addition, dysregulated bioactive lipid metabolism is also believed to be important. As an important AA-metabolizing enzyme, 5-LOX has been found to be markedly upregulated in stromal inflammatory cells and epithelial cells at the early stage of human OSCC^[52].

The gross observation in G1 (control: untreated animals) showed no observable gross changes, HBP mucosa appeared normal, the weak (7.05%) positive cytoplasmic expression of Bcl-2, in the basal and suprabasal epithelial layers, is in agreement with those of other investigators^[53-55]. The moderate (39.83%) cytoplasmic expression of Bax, in the superficial epithelial layer, is in agreement with those of other investigators^[55,56], these investigations stated that, under normal conditions, Bcl-2/ Bax ratio determines the fate of cell survival or cell death, through the regulation of the release of Cytochrome c from the mitochondria. This result may be due to that; Bcl-2 participates in the control of the terminal differentiation of keratinocytes by protecting their stem cells from apoptosis. In the present study epithelial dysplasia was observed After DMBA painting for 8 weeks (G2A), Finally, SCC formed after DMBA painting for 14 weeks (G2B). The activities of BCL2 were increased with the progression of HBP carcinogenesis. The strongest expressions (75.21%) were observed in malignant epithelium while the activities of Bax were decreased with the progression of HBP carcinogenesis, the weak expressions (10.45%) were observed in malignant epithelium and there was significant difference between (G1 and G2A), (G1 and G2B) respectively where P value was

(<0.05) regarding to Bcl2 expression and between (G1 and G2B) where P value was (<0.05) regarding to Bax expression. The trend observed in the present study was consistent with the results of previous studies^[57-59].

Under normal physiological conditions, free radicals are generated in subcellular compartments, which would subsequently be scavenged by antioxidant systems. DMBA carcinogen disrupts the pro-oxidant antioxidant balance, which finally leads to antioxidants depletion in cells (Li et al., 2002)^[60]. Krishnaveni and Mirunalini (2012)^[61] had reported decreased levels of lipid peroxidation (LPO) and antioxidants in tumor tissues, which could be due to prolonged tumour cells proliferation. Gross observation of G3A model revealed decrease in distribution and size of the nodules, ulcerative and bleeding areas compared to G2A at the same period, also in G3A reduced epithelial dysplasia incidence and severity of two premalignant lesions as compared to G2A, hyperkeratosis and moderate to severe dysplastic features in most epithelial layers in multiple areas including: loss of adhesion and abnormal mitosis with intact basement membrane while three specimen appeared normal almost the same as G1, Simultaneous treatment with I3C and DMBA in G3B significantly reduced OSCC incidence, the overlying epithelium in one animals of G3B (1 of 5) specimens has obvious dysplastic features in multiple areas with evidence of prominent true invasion with formation of epithelial nests. Well differentiated SCC nests were observed in the underlying C.T, while other 2 specimens exhibited severe dysplastic features without true invasion and 2 specimens exhibited mild dysplastic features without true invasion. In the present study in regard to expression of Bcl2 there was significant difference between (G2A and G3A) and between G2B and G3B respectively where P value was (<0.05) and there was no significant difference between G1 and G3A where P value was (0.718), Also In regard to Bax expression there was significant difference between G2B and G3B where P value was (<0.05) and there

was no significant difference between G1, G3B where P value was (0.464), decreased expressions of Bcl2 and increased expressions of cytochrome Bax in groups G3A and G3B suggested that the chemopreventive effect of I3C was accomplished by inhibiting tumor cell proliferation and inducing tumor cell apoptosis, this suggestion was consistent with the conclusions of previous in vitro studies [62-64,33].

Mounting evidence indicates that inactivation of Akt and its downstream effector, the nuclear transcription factor NF- κ B, plays a pivotal role in the proapoptotic action of I3C in tumor cells [65,66]. It is well documented that Akt promotes cell survival by stimulating NF- κ B signaling through I κ B α kinase in conjunction with the phosphorylating deactivation of several proapoptotic proteins including glycogen synthase kinase (GSK)3 β , Bad, Forkhead transcription factors, and caspase-9, thereby constituting an important target for cancer therapy [67]. NF- κ B acts as an important survival factor in cancer cells by mediating the transcription of a series of antiapoptotic genes, including: Bcl-2, Bcl-xL, survivin, p53, and p21 [68]. In addition, indole-3-carbinol has been shown to activate the stress-induced MAP kinases p38 and c-jun N-terminal kinase (JNK) in prostate cancer cells [69], and to inhibit constitutively active STAT3, a transcription factor, in pancreatic carcinoma cells [70]. Together, the concerted effects on these proapoptotic components underlie the ability of indole-3-carbinol/DIM to induce mitochondria-dependent apoptosis in tumor cells. The use of vegetables for hundreds of years, the hundreds of carefully observed animal studies, and the consumption of synthetic I3C by thousands of people without noticeable harmful effects have shown that I3C is a safe dietary supplement. Therefore, Indole-diet derivatives were found to be safe compounds and they were evaluated in human clinical trials as potential chemopreventive agents. In phase I trial of I3C, 17 women from a high-risk breast cancer were used [71].

CONCLUSIONS

From the results of the present study the following conclusions could be drawn: I3C is considered as a promising chemotherapeutic agent in prevention of induced HBP carcinogenesis (epithelial dysplasia & invasive carcinoma) and proved beneficial role in improving the outcome by modulating apoptosis and proliferation throughout the process of carcinogenesis.

REFERENCES

1. Williams H. K. Molecular pathogenesis of oral squamous carcinoma. *Molecular Pathology* 2000; 53: 165-72.
2. Jemal A, Siegel R, Ward E, Hao Y, Xu J, Thun M. Cancer statistics, *CA Cancer Journal for Clinicians* 2009; 59: 225-49.
3. Parkin D, Laara E, Muir C. Estimates of the worldwide frequency of sixteen major cancers in 1980. *International Journal of Cancer* 1988; 41: 184-97.
4. Matsuda T, Marugame T, Kamo K, Katanoda K, Ajiki W, Sobue T. Cancer incidence and incidence rates in Japan in 2003: based on data from 13 population-based cancer registries in the monitoring of cancer incidence in Japan (MCIJ) project," *Japanese Journal of Clinical Oncology* 2009; 39:850-58.
5. Boffetta P, Hecht S, Gray N, Gupta P, Straif K. Smokeless tobacco and cancer. *The Lancet Oncology* 2008; 9: 667-75.
6. Scholes AG, Woolgar JA, Boyle MA, Brown JS, Vaughan ED, Hart CA, et al. Synchronous oral carcinomas: independent or common clonal origin. *Cancer Res* 1998; 58:2003-06.
7. Califano J, Westra WH, Meininger G, Corio R, Koch WM, Sidransky D. et al. Genetic progression and clonal relationship of recurrent premalignant head and neck lesions. *Clin Cancer Res* 2000;6: 347-52.
8. Weber RG, Scheer M, Born IA, Joos S, Cobbers JM, Hofele C, et al. Recurrent chromosomal imbalances detected in biopsy material from oral premalignant and malignant lesions by combined tissue microdissection, universal DNA amplification, and comparative genomic hybridization. *Am J Pathol* 1998; 153: 295-303.
9. Sudbø J, Kildal W, Risberg B. DNA content as a prognostic marker in patients with oral leukoplakias. *N Engl J Med* 2001;344: 1270-78.

10. Manoharan S, Vasanthaselman M, Silvan S, Baskaran N, Kumar S, Vinoth K. Carnosic acid a potent chemopreventive agent against oral carcinogenesis. *J Chem Biol Interact* 2010; 188: 616-22.
11. Taghavi N, Yazdi I. Prognostic factors of survival rate in oral squamous cell carcinoma: Clinical, histologic, genetic and molecular concepts. *Arch Iran Med* 2015; 18: 314 -19.
12. Vermorken JB, Remenar E, van Herpen C, Gorlia T, Mesia R, Degardin M, et al. Cisplatin, fluorouracil and docetaxel in unresectable head and neck cancer. *N Engl J Med* 2007; 357: 1695- 704.
13. Singh RP, Tyagi AK, Dhanalakshmi S, Agarwal R, Agarwal C. Grape seed extract inhibits advanced human prostate tumor growth and angiogenesis and upregulates insulin-like growth factor binding protein-3. *Int J Cancer* 2004; 108:733-40.
14. Silalahi J. Anticancer and health protective properties of citrus fruit components. *Asia Pac J Clin Nutr* 2002;79: 84-11:79.
15. Yao LH, Jiang YM, Shi J, Tomas-Barberan FA, Datta N, Singanusong R, et al. Flavonoids in food and their health benefits. *Plant Foods Hum Nutr* 2004; 59:113-22.
16. Chen MS, Chen D, Dou QP. Inhibition of proteasome activity by various fruits and vegetables is associated with cancer cell death. *In Vivo* 2004; 18:73-80.
17. Temple NJ, Gladwin KK. Fruit, vegetables, and the prevention of cancer: research challenges. *Nutrition* 2003; 19:467-70.
18. Steinmetz KA, Potter JD. Vegetables, fruit, and cancer prevention: a review. *J Am Diet Assoc* 1996; 96:1027-39.
19. Lewis S, Brennan P, Nyberg F, Ahrens W, Constantinescu V, Mukeria A, et al. Cruciferous vegetable intake, GSTM1 genotype and lung cancer risk in a non-smoking population. *IARC Sci Publ* 2002; 507:156-58.
20. Witte JS, Longnecker MP, Bird CL, Lee ER, Frankl HD, Haile RW. Relation of vegetable, fruit, and grain consumption to colorectal adenomatous polyps. *Am J Epidemiol* 1996;144:1015 -25.
21. Kristal AR, Lampe JW. Brassica vegetables and prostate cancer risk: a review of the epidemiological evidence. *Nutr Cancer* 2002; 42:1-9.
22. Fowke JH, Chung FL, Jin F, Qi D, Cai Q, Conaway C, et al. Urinary isothiocyanate levels, brassica, and human breast cancer. *Cancer Res* 2003;63:3980- 86.
23. Grubbs CJ, Steele VE, Casebolt T, Juliana MM, Eto I, Whitaker LM, et al. Chemoprevention of chemically-induced mammary carcinogenesis by indole-3-carbinol. *Anticancer Res* 1995; 15:716- 09.
24. Bradlow HL, Michnovicz J, Telang NT, Osborne MP. Effects of dietary indole-3-carbinol on estradiol metabolism and spontaneous mammary tumors in mice. *Carcinogenesis* 1991; 12. 1571-74.
25. Zhu CY, Loft S. Effect of chemopreventive compounds from Brassica vegetables on NAD(P)H:quinone reductase and induction of DNA strand breaks in murine hepa1c1c7 cells. *Food Chem Toxicol* 2003; 41:455-62.
26. Pappa G, Strathmann J, Löwinger M, Bartsch H, Gerhäuser C. Quantitative combination effects between sulforaphane and 3,3'-diindolylmethane on proliferation of human colon cancer cells in vitro. *Carcinogenesis* 2007; 28: 1471- 77.
27. Tadi K, Chang Y, Ashok BT, Chen Y, Moscatello A. 3,3'-Diindolylmethane, a cruciferous vegetable derived synthetic antiproliferative compound in thyroid disease. *Bioch Biophys Res Commun* 2005; 337: 1019-25.
28. Abdelrahim M, Ewman K, Vanderlaag K, Samudio I, Safe S. 3,3'-diindolylmethane (DIM) and its derivatives induce apoptosis in pancreatic cancer cells through endoplasmic reticulum stress-dependent upregulation of DR5. *Carcinogenesis* 2006; 27: 717-28.
29. Oganessian A, Hendricks JD, Williams DE. Long term dietary indole-3- carbinol inhibits diethylnitrosamine-initiated hepatocarcinogenesis in the infant mouse model. *Cancer Lett* 1997; 118: 87-94.
30. Savino JA, Evans JF, Rabinowitz D, Auborn KJ, Carter TH. Multiple, disparate roles for calcium signaling in apoptosis of human prostate and cervical cancer cells exposed to diindolylmethane. *Mol Cancer Ther* 2006; 5: 556-63.
31. Kim DS, Jeong YM, Moon SI, Kim SY, Kwon SB. Indole-3-carbinol enhances ultraviolet B-induced apoptosis by sensitizing human melanoma cells. *Cell Mol Life Sci* 2006; 63: 2661-68.
32. Qian X, Melkamu T, Upadhyaya P, Kassie F. Indole-3-carbinol inhibited tobacco smoke carcinogen-induced lung adenocarcinoma in A/J mice when administered during the post-initiation or progression phase of lung tumorigenesis. *Cancer Lett* 2011; 311: 57-65.
33. Young S., Milner J. Targets for indole-3-carbinol in cancer prevention. *Journal of Nutritional Biochemistry* 16 2005 65-73

34. Anon, A. A clinical development plan: indole-3-carbinol. *J. Cell. Biochem* 1996; 26: 127–36.
35. Grose, K, Bjeldanes, L. Oligomerization of indole-3-carbinol in aqueous acid. *Chem. Res. Toxicol* 1992; 5: 188–93.
36. Aggarwal BB. Nuclear factor-kappaB: the enemy within. *Cancer Cell* 2004; 6: 203–8.
37. Weng JR, Tsai CH, Kulp SK, Wang D, Lin CH, Yang HC, et al. A potent indole-3-carbinol derived antitumor agent with pleiotropic effects on multiple signaling pathways in prostate cancer cells. *Cancer Res* 2007; 67: 7815–24.
38. Lian JP, Word B, Taylor S, Hammons GJ, Lyn-Cook BD. Modulation of the constitutive activated STAT3 transcription factor in pancreatic cancer prevention: effects of indole-3-carbinol (I3C) and genistein. *Anticancer Res* 2004; 24: 133–37.
39. James A, John G, Barry S, Michael J, Charles D. Indole-3-carbinol, but not its major digestive product 3,3V-diindolylmethane, induces reversible hepatocyte hypertrophy and cytochromes P450. *Toxicology and Applied Pharmacology* 2006; 211: 115 –23.
40. Negi A, Puri A, Gupta R, Nangia R, Sachdeva A, Mittal M. Comparison of immunohistochemical expression of antiapoptotic protein survivin in normal oral mucosa, oral leukoplakia, and oral squamous cell carcinoma. *Patholog Res Int* 2015; 2015:1-6.
41. Gimenez-Conti I.B. The hamster cheek pouch carcinogenesis model. *J. Cell Biochem* 1993, 53: 83–90.
42. Morris A.L. Factors influencing experimental carcinogenesis in the hamster cheek pouch. *J. Dent. Res* 1961; 40: 3–15.
43. Kim S. A., Ahn S. G., Kim D. K., Kim S. G., Lee S. H., Kim J., et al. Sequential expression of inducible nitric oxide synthase and cyclooxygenase-2 during DMBA-induced hamster buccal pouch carcinogenesis. *In Vivo*, 2004 18, 609–14.
44. Lajolo C., Giuliani M., Sgambato A., Majorano E., Lucchese A., Capodiferro Favia G. N-(4-hydroxyphenyl) all-trans-retinamide (4-HPR) high dose effect on DMBA-induced hamster oral cancer: a histomorphometric evaluation. *International Journal of Oral and Maxillofacial Surgery* 2008; 37: 1133–40.
45. Nishimura N., Urade M., Hashitani S., Noguchi K., Manno Y., Takaoka K., et al. Increased expression of cyclooxygenase (COX)-2 in DMBA-induced hamster cheek pouch carcinogenesis and chemopreventive effect of a selective COX-2 inhibitor celecoxib. *Journal of Oral Pathology and Medicine* 2004; 33: 614–21.
46. Manoharan S, Vasanthaselvan M, Silvan S, Baskaran N, Kumar S, Vinoth K. Carnosic acid a potent chemopreventive agent against oral carcinogenesis. *J Chem Biol Interact* 2010; 188: 616-22.
47. Manoharan S, Singh A, Suresh K, Vasudevan K, Subhasini R, Baskaran N. Anti-tumor initiating potential of andrographolide in 7, 12-dimethylbenz[a]anthracene induced hamster buccal pouch carcinogenesis. *J Asian Pac Cancer Prev* 2012;13:5701-8.
48. Singh A, Manoharan S, Suresh K. Modulating effect of andrographolide on cell surface glycoconjugates status during 7, 12-dimethylbenz(a)anthracene induced hamster buccal pouch carcinogenesis. *J Int Res Pharm Sci* 2012; 3: 200-5.
49. Monti A, Aromando R, Pérez M, Schwint A, Itoiz M. The hamster cheek pouch model for field cancerization studies. *J Periodontol* 2000, 2015; 67: 292-311.
50. Chen, Y.K. Correlation between inducible nitric oxide synthase and p53 expression for DMBA-induced hamster buccal-pouch carcinomas. *Oral Dis* 2003; 9: 227–34.
51. Chen, Y.K. Increased expression of inducible nitric oxide synthase in human oral submucous fibrosis, verrucous hyperplasia, and verrucous carcinoma. *Int. J. Oral Maxillofac. Surg* 2002; 31: 419–22.
52. Sood, S. Overexpression of 5-lipoxygenase and cyclooxygenase 2 in hamster and human oral cancer and chemopreventive effects of Zileuton and celecoxib. *Clin. Cancer Res* 2005; 11: 2089–96.
53. Kathiresan S, Mariadoss A, Muthusamy R, Kathiresan S. Protective effects of [6]-shogaol on histological and immunohistochemical gene expression in DMBA induced hamster buccal pouch carcinogenesis. *J Asian Pacific Cancer Prev* 2013; 14:3123-29.
54. Balakrishnan S, Manoharan S, Alias L, Nirmal M. Effect of curcumin and ferulic acid on modulation of expression pattern of p53 and bcl-2 proteins in 7, 12-dimethylbenz anthracene-induced hamster buccal pouch carcinogenesis. *J Indian Biochem Biophys* 2010;47:7-12.
55. Rajasekaran D, Manoharan S, Silvan S, Vasudevana K, Baskaran N, Palanimuthu D. Proapoptotic, anti-cell proliferative, anti-inflammatory and antiangiogenic potential of carnosic acid during 7, 12 dimethylbenz [a] anthracene-induced hamster buccal pouch carcinogenesis. *J Afr Tradit Complement Altern Med* 2013;10: 102–12.

56. Manoharan S, Palanimuthu D, Baskaran N, Silvan S. Modulating effect of lupeol on the expression pattern of apoptotic markers in 7,12-dimethylbenz(a)anthracene induced oral carcinogenesis. *J Asian Pac Cancer Prev* 2012; 13: 5753-57.
57. Zhang W, Yin G, Dai J, Sun YU, Hoffman RM, Yang Z, et al. Chemoprevention by Quercetin of Oral Squamous Cell Carcinoma by Suppression of the NF-kb Signaling Pathway in DMBA-treated Hamsters. *Anticancer Res* 2017;37: 4041-49.
58. Yang P, Sun Z, Chan D, Cartwright CA, Vijjeswarapu M, Ding J, et al. Zylflamend_ reduces LTB4 formation and prevents oral carcinogenesis in a 7,12-dimethylbenz[a]anthracene (DMBA)-induced hamster cheek pouch model. *Carcinogenesis* 2008; 29: 2182-89.
59. Kathiresan S, Govindhan A. [6]-Shogaol, a Novel Chemopreventor in 7,12-Dimethylbenz[a]anthracene-induced Hamster Buccal Pouch Carcinogenesis. *Phytother Res* 2016; 30:646-53.
60. Li N, Chen X, Liao J, Yang G. Inhibition of 7,12 dimethylbenz[a]anthracene (DMBA) induced oral carcinogenesis in hamsters by tea and curcumin. *Carcinogenesis* 2002; 23: 1307-13.
61. Krishnaveni M, Mirunalini S. Chemopreventive efficacy of *Phyllanthus emblica* L. (amla) fruit extract on 7,12-dimethylbenz(a)anthracene induced oral carcinogenesis- A dose-response study. *Environ Toxicol Pharmacol* 2012; 34: 801-10.
62. Ben L, Theodor F. Indole-3-carbinol: A glucosinolate derivative from cruciferous vegetables for prevention and complementary treatment of breast cancer. *Gemüsen Deutsche Zeitschrift für Onkologie* 2015; 47: 20-27
63. Jing-Ru Weng, Chen-Hsun Tsai, Samuel K. Kulp, Ching-Shih Chen. Indole-3-carbinol as a chemopreventive and anti-cancer agent. *Cancer Lett* 2008; 262: 153-58.
64. Sundar SN1, Kerekatte V, Equinozio CN, Doan VB, Bjeldanes LF, Firestone GL. Indole-3-Carbinol Selectively Uncouples Expression and Activity of Estrogen Receptor Subtypes in Human Breast Cancer Cells. *Mol Endocrinol* 2006 ;20: 3070-82.
65. Rahman KW, Sarkar FH. Inhibition of nuclear translocation of nuclear factor- κ B contributes to 3,3'-diindolylmethane-induced apoptosis in breast cancer cells. *Cancer Res* 2005;65: 364-71.
66. Takada Y, Andreeff M, Aggarwal BB. Indole-3-carbinol suppresses NF-kappaB and IkappaBalpha kinase activation, causing inhibition of expression of NF-kappaB-regulated antiapoptotic and metastatic gene products and enhancement of apoptosis in myeloid and leukemia cells. *Blood* 2005;106:641-49.
67. Yoeli-Lerner M, Toker A. Akt/PKB signaling in cancer: a function in cell motility and invasion. *Cell Cycle* 2006;5:603-5.
68. Aggarwal BB. Nuclear factor-kappaB: the enemy within. *Cancer Cell* 2004;6:203-208.
69. Weng JR, Tsai CH, Kulp SK, Wang D, Lin CH, Yang HC, et al. A potent indole-3-carbinol derived antitumor agent with pleiotropic effects on multiple signaling pathways in prostate cancer cells. *Cancer Res* 2007;67:7815-24.
70. Lian JP, Word B, Taylor S, Hammons GJ, Lyn-Cook BD. Modulation of the constitutive activated STAT3 transcription factor in pancreatic cancer prevention: effects of indole-3-carbinol (I3C) and genistein. *Anticancer Res* 2004;24:133-37.
71. Reed GA, Peterson KS, Smith HJ, Gray JC, Sullivan DK. A phase I study of indole-3-carbinol in women: tolerability and effects. *Cancer Epidemiol Biomarkers Prev* 2005; 14: 1953-60.